AD-A052 841 AEROSPACE CORP EL SEGUNDO CALIF SPACE SCIENCES LAB F/G 20/9

ION CYCLOTRON WAVES GENERATED BY AN IONOSPHERIC BARIUM INJECTIO--ETC(U)

MAR 78 H C KOONS, M B PONGRATZ F04701-77-C-0078

UNCLASSIFIED TR-0078(3960-06)-1 SAMSO-TR-78-66 NL

| OF |

AD
A052841

END

DATE
FILMED

6-78

DDC

REPORT SAMSO-TR-78-66

Ion Cyclotron Waves Generated by an Ionospheric Barium Injection

H. C. KOONS
Space Sciences Laboratory
The Ivan A. Getting Laboratories
The Aerospace Corporation
El Segundo, Calif. 90245
and
M. B. PONGRATZ
University of California
Los Alamos Scientific Laboratory
Los Alamos, New Mexico 87545

13 March 1978

Interim Report

Prepared for
SPACE AND MISSILE SYSTEMS ORGANIZATION
AIR FORCE SYSTEMS COMMAND
Los Angeles Air Force Station
P.O. Box 92960, Worldway Postal Center
Los Angeles, Calif. 90009

This interim report was submitted by The Aerospace Corporation, El Segundo, CA 90245, under Contract No. F04701-77-C-0078 with the Space and Missile Systems Organization, Deputy for Advanced Space Programs, P.O. Box 92960, Worldway Postal Center, Los Angeles, CA 90009. It was reviewed and approved for The Aerospace Corporation by G. A. Paulikas, Director, Space Sciences Laboratory. Lieutenant Dara Batki, SAMSO/YCPT, was the project officer for Advanced Space Programs.

This report has been reviewed by the Information Office (OI) and is releasable to the National Technical Information Service (NTIS). At NTIS, it will be available to the general public, including foreign nations.

This technical report has been reviewed and is approved for publication. Publication of this report does not constitute Air Force approval of the report's findings or conclusions. It is published only for the exchange and stimulation of ideas.

Dara Batki

Dara Batki, Lt, USAF
Project Officer

Robert W. Lindemuth

Robert W. Lindemuth, Lt Col, USAF
Chief, Technology Plans Division

FOR THE COMMANDER

Leonard E. Baltzell

LEONARD E. BALTZELL, Col, USAF
Asst. Deputy for Advanced Space Programs

UNCLASSIFIED

SECURITY CLASSIFICATION OF THIS PAGE (When Data Entered)

19 **REPORT DOCUMENTATION PAGE**

READ INSTRUCTIONS BEFORE COMPLETING FORM

1. REPORT NUMBER: 18 SAMSO TR-78-66	2. GOVT ACCESSION NO.
3. RECIPIENT'S CATALOG NUMBER	
4. TITLE (and Subtitle): 6 ION CYCLOTRON WAVES GENERATED BY AN IONOSPHERIC BARIUM INJECTION.	5. TYPE OF REPORT & PERIOD COVERED: 9 Interim rept.
	6. PERFORMING ORG. REPORT NUMBER: 14 TR-0078(3960-06)-1
7. AUTHOR(s): 10 Harry C. Koons [redacted] Morris B. Pongratz	8. CONTRACT OR GRANT NUMBER(s): 15 F04701-77-C-0078
9. PERFORMING ORGANIZATION NAME AND ADDRESS: The Aerospace Corporation, El Segundo, Calif. 90245	10. PROGRAM ELEMENT, PROJECT, TASK AREA & WORK UNIT NUMBERS
11. CONTROLLING OFFICE NAME AND ADDRESS: Space and Missile Systems Organization, Air Force Systems Command, Los Angeles, Calif. 90009	12. REPORT DATE: 11 13 Mar [redacted] 78
	13. NUMBER OF PAGES: 25 12 24p.
14. MONITORING AGENCY NAME & ADDRESS (if different from Controlling Office)	15. SECURITY CLASS. (of this report): Unclassified
	15a. DECLASSIFICATION/DOWNGRADING SCHEDULE

16. DISTRIBUTION STATEMENT (of this Report)

Approved for public release; distribution unlimited.

17. DISTRIBUTION STATEMENT (of the abstract entered in Block 20, if different from Report)

18. SUPPLEMENTARY NOTES

19. KEY WORDS (Continue on reverse side if necessary and identify by block number)

Barium Injection
Ionosphere
Ion Cyclotron Waves
Plasma Instabilities

20. ABSTRACT (Continue on reverse side if necessary and identify by block number)

A shaped-charge, barium, plasma-injection experiment was performed in June 1976 at the ERDA Kauai Test Facility. The barium was injected perpendicular to the geomagnetic field at an altitude of 450 km. The second stage of the rocket, located approximately 1.2 km from the point of detonation, contained a payload to measure dc and ac electric fields using a dual spherical-probe antenna. A variety of plasma waves were detected for approximately 20 sec following the detonation. The initial impulse generated

next page

DD FORM 1473 (FACSIMILE)

407 512 JOB

UNCLASSIFIED

SECURITY CLASSIFICATION OF THIS PAGE (When Data Entered)

UNCLASSIFIED

SECURITY CLASSIFICATION OF THIS PAGE(When Data Entered)

19. KEY WORDS (Continued)

$O_2^{(+)}$,

20. ABSTRACT (Continued)

ion cyclotron waves at the $Ba^{(+)}$, $O_2^{(+)}$, $Al^{(+)}$, $OH^{(+)}$, and $O^{(+)}$ gyrofrequencies. This was followed by a time period during which ion cyclotron waves were observed in passbands between the barium gyrofrequency harmonics up to the oxygen gyrofrequency. At the high frequency end of this range of the spectrum is essentially continuous, i.e., similar to an ion sound wave spectrum.

UNCLASSIFIED

SECURITY CLASSIFICATION OF THIS PAGE(When Data Entered)

PREFACE

We are grateful to D. C. Pridmore-Brown for the computer calculations. We are also grateful to Bob Jeffries, the Buaro project leader, at the Los Alamos Scientific Laboratories and to Al Huters, Herman Wente John Moyer and Win Watson of Sandia Laboratories, Albuquerque, and W. B. Harbridge and C. W. Jordan of The Aerospace Corporation for their efforts in assembling and launching the rocket and payloads.

CONTENTS

FIGURES

I. INTRODUCTION

The explosion of small barium canisters in the ionosphere stimulates a variety of plasma waves associated with both micro- and macro-instabilities. Electric-field fluctuations near and below the oxygen ion gyrofrequency and electric-field and plasma-density fluctuations at frequencies above the oxygen ion gyrofrequency were observed in a series of barium release experiments in the ionosphere at auroral latitudes by Kelley et al.[1] They suggest that the lowest-frequency modes might be Alfven waves, drift waves, or electrostatic acoustic waves.

In this paper we report ac electric field measurements made in this same frequency range during a large barium injection at middle latitude. The waves are identified as ion cyclotron waves with dominant spectral peaks occuring at the barium gyrofrequency and at the gyrofrequencies of O^+, O_2^+, OH^+, and Al^+ shortly after the explosion. This is followed by a time period exhibiting a broadband spectrum below the O^+ gyrofrequency. This spectrum is characterized by attenuation bands at the barium gyrofrequency and its harmonics.

II. DESCRIPTION OF THE EXPERIMENT

A shaped-charge, barium, plasma-injection experiment (code named Buaro) was performed in June 1976 at the ERDA Kauai Test Facility by The Los Alamos Scientific Laboratory. The rocket payload contained seven shaped charges, a sevenfold larger package than the typical payloads employed in previous barium plasma injections conducted in this program. An attitude control system oriented the injection perpendicular to the local geomagnetic field. The injection occurred at an altitude of 450 km within a couple of seconds of rocket apogee. The ambient electron density at this altitude was $\sim 3 \times 10^4$ cm^{-3}.

The seven shaped charges were arranged in a cluster containing six equally spaced on the circumference of a circle with the seventh at the center of the circle. Inside each charge was a metal cone containing 1450 g of barium. Assuming that about 30% of the barium was shock vaporized, approximately 1.3×10^{25} barium atoms were released. Of this, about half would be in the directed beam of fast atoms. The remainder would be in a spherically expanding cloud of thermal atoms. Figure 1 shows the expected neutral barium velocity distribution.

The second stage of the rocket contained a payload furnished by The Aerospace Corporation to measure ac and dc electric fields using a 5-m long tip-to-tip dual spherical probe antenna. The "dc" electric field measurement has two voltage ranges ± 200 mV and ± 400 mV peak-to-peak and had a frequency response from dc to 160 Hz.

The upper section containing the barium-lined shaped charges was spring ejected from the second stage containing the electric-field experiment approximately four minutes before the canisters were detonated. The separation velocity was approximately

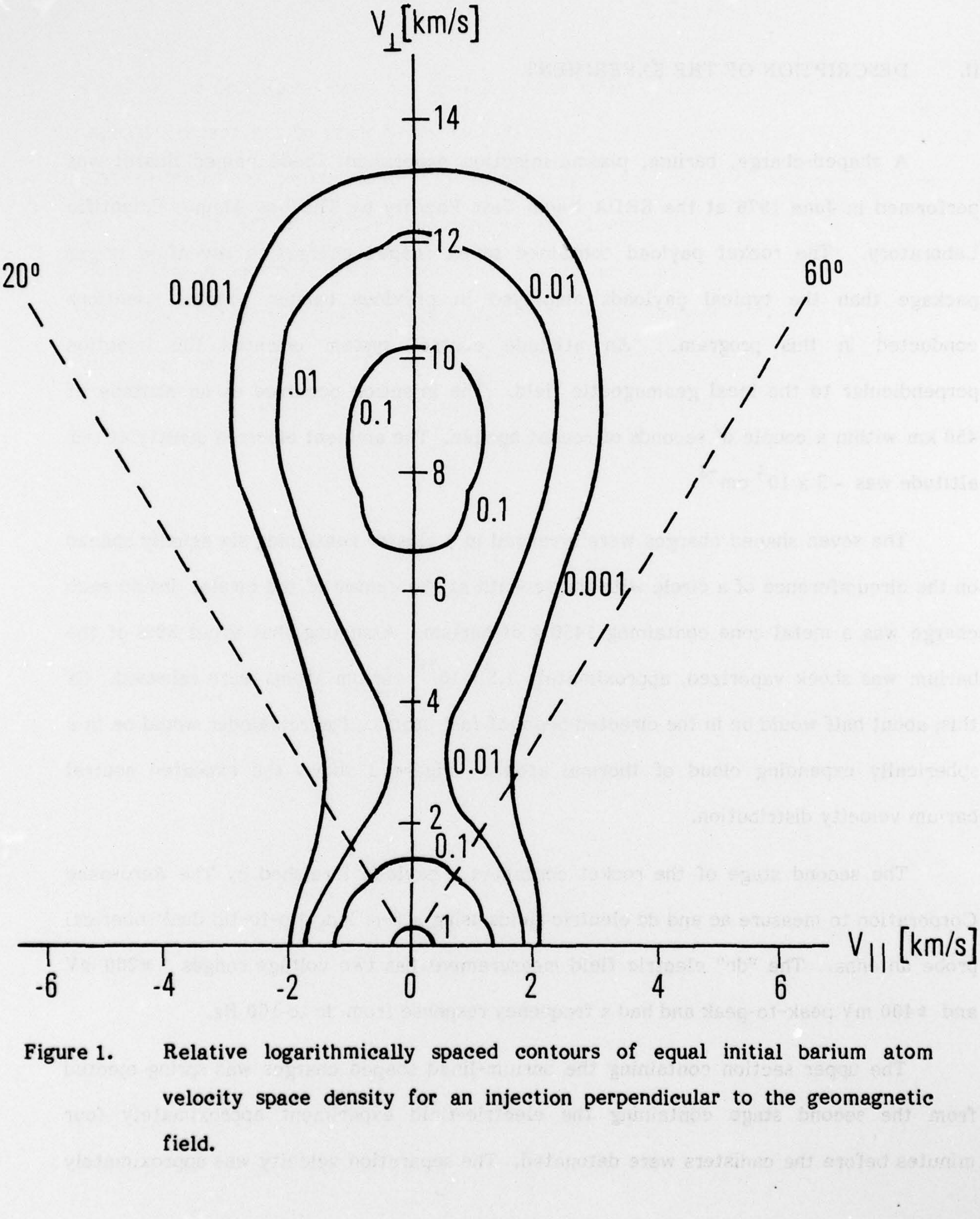

Figure 1. **Relative logarithmically spaced contours of equal initial barium atom velocity space density for an injection perpendicular to the geomagnetic field.**

5 m/sec, placing the second stage about 1.2 km behind the upper stage and on the same trajectory at the time of detonation. Since the center of mass of the thermal barium distribution generally followed the trajectory of the upper stage, the electric-field measurements were made at essentially the same point relative to the center of the barium thermal distribution throughout the measurement period described in this paper. During the first 20 sec the barium neutral distribution expands with a gaussian shape with the radius increasing at a mean velocity of 1.75 km/sec. The expansion was generally isotropic with somewhat more mass moving backwards than forwards. The mean ionization time for a barium atom is 19 sec.

III. CHEMISTRY

The detonation of the explosive produces H_2O and CO_2 in vapor phase. As described by Pongratz et al.[3] these molecules charge exchange rapidly with O^+ the dominant ambient ion. Likely ion producing reactions are:

A. Water Vapor

$$H_2O + O^+ \rightarrow H_2O^+ + O$$

$$H_2O^+ + H_2O \rightarrow H_3O^+ + OH$$

$$OH + O^+ \rightarrow OH^+ + O$$

B. Carbon Dioxide

$$CO_2 + O^+ \rightarrow O_2^+ + CO$$

$$\rightarrow CO_2^+ + O$$

$$O_2^+ + N \rightarrow NO^+ + O$$

Photoionization of explosion produced vapors of the metals aluminum and barium produce Al^+ and Ba^+. The rocket framework and skin were made of aluminum.

IV. OBSERVATIONS

A. Spectra

A variety of plasma waves were detected for approximately 20 sec following the detonation. In this paper, we will only describe those that were detected below the oxygen grofrequency. The analog record from the "dc" channel is shown in Figure 2. The detonation occurred at 1430:01.266 UT, June 7, 1976.

The analog data (Figure 2) were digitized at a sample rate of 500 samples per second and spectrum analyzed in three-second intervals using a fast fourier-transform technique employing a Hanning lag window.[2] The power spectral density is calculated at 0.33 Hz intervals and the effective bandwidth is 1.11 Hz.

The spectrum during the three-second interval immediately following the detonation is shown in Figure 3a. The dominant peak at the low frequency end occurs at 3.33 Hz and corresponds with the barium gyrofrequency which is 3.34 Hz in the 0.3 G geomagnetic field at the detonation altitude.

Several other emission lines are identified in the spectrum. Identification of these lines is complicated by possible contamination from noise signals that were present before the detonation.

B. Background

A background spectrum obtained from the three-second interval preceding the detonation is shown in Figure 4. The total dynamic range of the measurement is about 50 dB. The largest amplitude peak at 1.0 Hz corresponds with the spin rate of the vehicle.

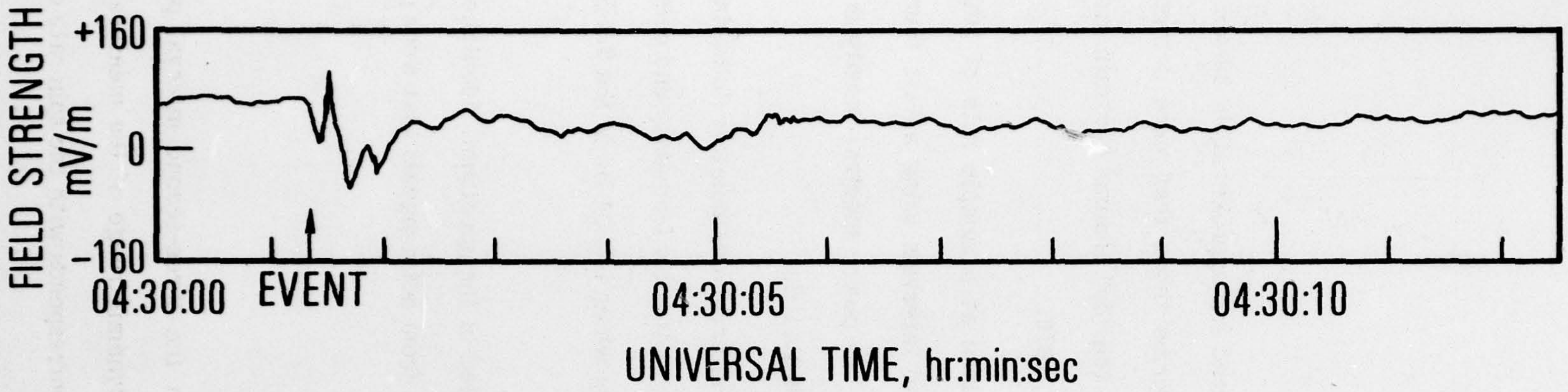

Figure 2. Electric field measured by the dual spherical probe antenna. The time of the barium injection is identified by the arrow.

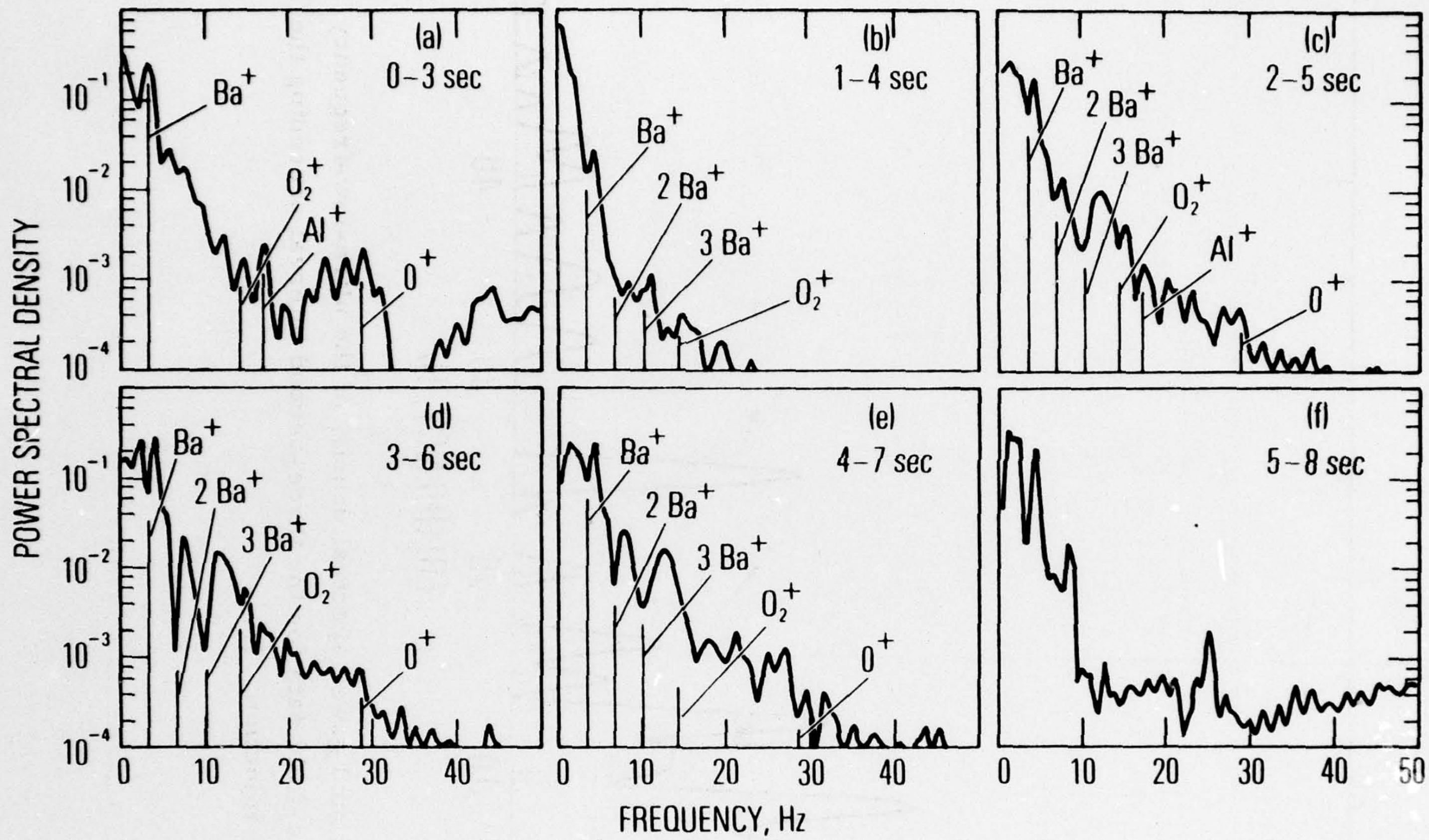

Figure 3. Power spectral density of the ultra-low-frequency electric-field data for selected three-second intervals following the barium injection. The time period with respect to the injection is identified on each graph. Ion gryofrequencies and the harmonics of the barium ion gyrofrequency are identified by vertical lines.

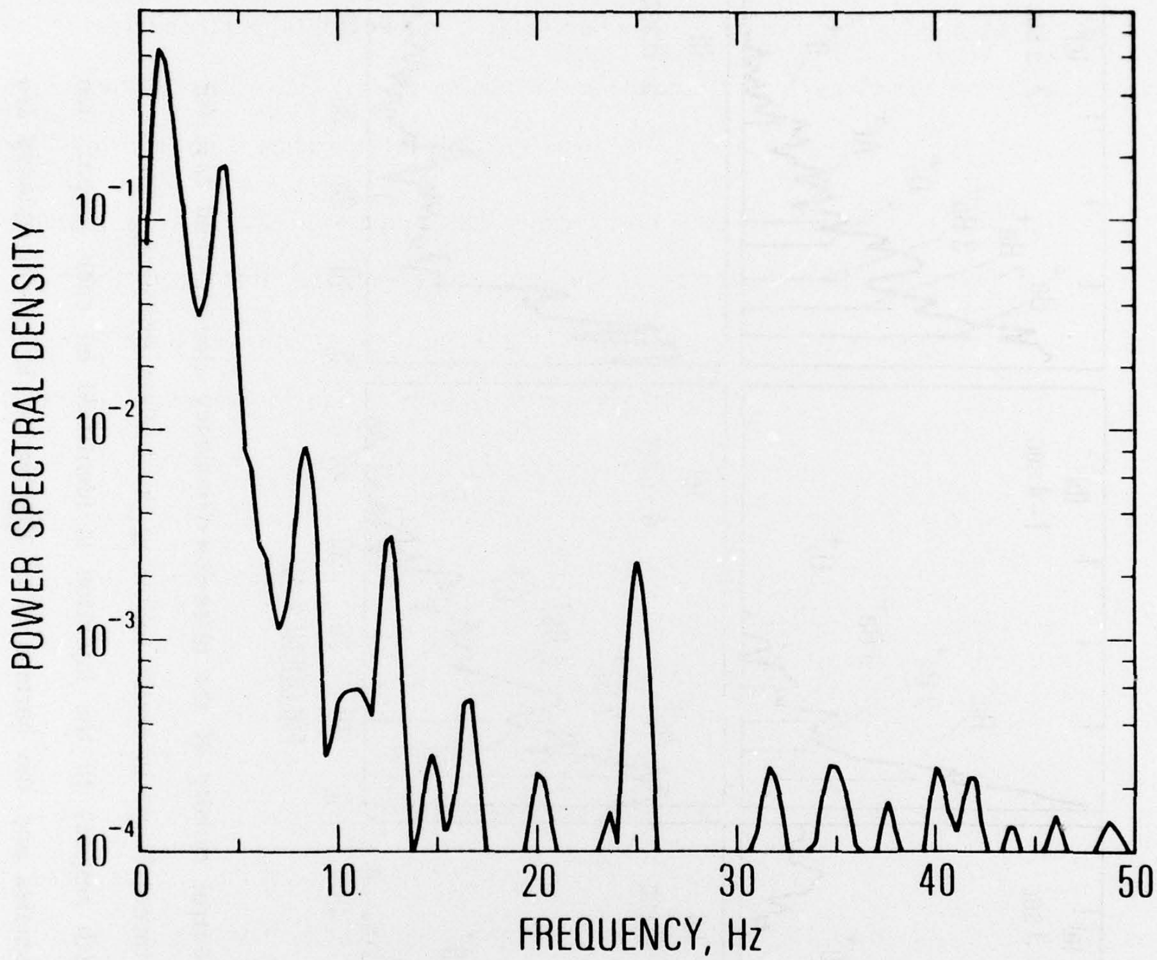

Figure 4. Background power spectral density of the ultra-low-frequency electric-field data for the three-second interval preceding the barium injection.

Within the accuracy of the analysis the peaks at 4.33, 8.33, 12.67, 16.67, 20.00, and 25.00 Hz are harmonically related. The fundamental frequency obtained by averaging the fundamental frequencies derived from these harmonics is 4.17 Hz. This is the fourth harmonic of the rocket spin frequency. The source of this interference is not known.

A significant amount of this interference is suppressed for a few seconds immediately following the detonation. The amplitudes of the third and the sixth harmonics are plotted as a function of time in Figure 5. The amplitudes were obtained from power spectral density calculations for partially overlapping three-second intervals including those shown in Figure 3. The fundamental at 4.33 Hz and the second harmonic showed similar temporal behavior to the sixth harmonic. The third and fourth harmonics behaved similarly. The fifth harmonic was too low in amplitude to characterize.

C. Temporal Evolution

The temporal evolution of the plasma wave spectrum is shown in Figure 3. The interval immediately following the detonation (Figure 3a) is characterized by a series of identifiable emission peaks at gyrofrequencies associated with oxygen ions and detonation product ions. The next interval (Figure 3b) is characterized by a sharp decrease in the spectral density with increasing frequency. The spectral density is generally less than the predetonation spectrum and significantly less than the interval immediately after the detonation. The spectrum is also quite smooth with little evidence of the harmonically related interference frequencies or gyrofrequency emissions. This period corresponds with the time of minimum amplitude for the interference peaks.

The intervals comprising the time from 2 to 7 sec after the detonation are characterized by a broadband spectrum extending from below the barium gyrofrequency at 3.3 Hz to just above the oxygen gyrofrequency at 28.6 Hz. The most notable feature of

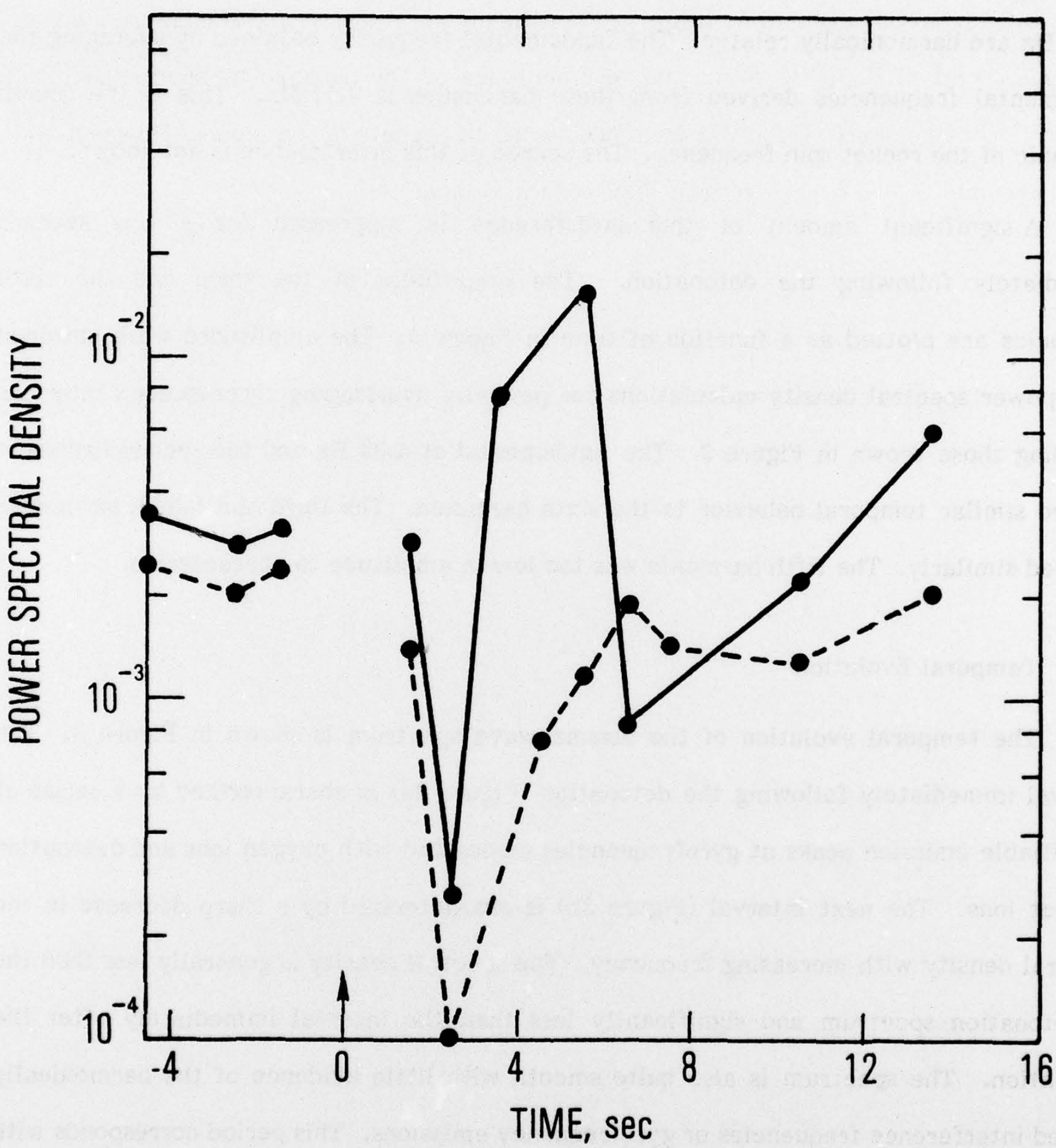

Figure 5. Temporal behavior of the background interference lines at 12.67 Hz (solid curve) and 25.00 Hz (dashed curve).

these spectra is stopbands at the barium gyrofrequency and its first and second harmonics. The last interval in Figure 3 shows the re-emergence of the background spectrum. The first and fifth harmonics of 4.17 Hz have recovered to predetonation levels. However the second harmonic is still supressed (See Figure 4 for comparison).

V. INTERPRETATION

A. Ion Cyclotron Emissions

The general solution to the wave equation in a temperate inhomogeneous plasma has resonances, i.e. the index of refraction beomes very large, as $\omega \rightarrow \Omega_{ci}$ where Ω_{ci} is the gyrofrequency for each type of ion, i. The barium detonation is represented by a discontinuity in the input function. With a delta function or unit impulse as the driving function, the specific solution to the wave equation will again contain resonances as $\omega \rightarrow \Omega_{ci}$. The system behavior is analogous to a bell that is hit with a hammer. The bell emits acoustic waves at its resonance frequency and overtones.

Thus, immediately after the detonation, emissions are expected at the gyrofrequencies of the ions present in the plasma. In the three-second interval immediately following the detonation, the spectrum contains emission lines at the gyrofrequencies of Ba^+, O_2^+, Al^+, OH^+, and O^+. These are identified in Figure 3a. It is impossible to determine if the line at 25 Hz immediately following the detonation (Figure 3a) is an emission line or the remnants of the noise line. The frequency is very nearly the gyrofrequency for a water vapor ion. Approximately 2000 mols of water vapor were producted in the detonation.[3]

B. Ion Cyclotron Instability

A quiet interval (Figure 3b) follows the detection of the impulse-generated emissions at the ion gyrofrequencies. This quiet interval is followed by several seconds of emissions below the oxygen gyrofrequency. The spectra for this time period shown in

Figures 3c-3e show clear pass bands bounded by the barium gyrofrequency and its harmonics. The theory of ion-cyclotron instabilities predicts a narrow band of unstable frequencies just above $\omega = n\ \Omega_{ci}$ for perpendicular propagation.

In laboratory experiments[4-6] waves destablized by a parallel electron current first appear near $\omega = 1.2\ \Omega_{ci}$. With further increases in the drift velocity, the instability develops harmonics and finally a continuous spectrum evolves.[6]

In Figures 3b-3c, the peak in the spectra just above the barium gyrofrequency maximizes at 4.33 Hz, i.e. $\omega = 1.3\ \Omega_{ci}$, but is essentially of equal amplitude between 4.0 and 4.33 Hz, i.e. ω between 1.2 Ω_{ci} and 1.3 Ω_{ci}. Although it might be argued that this peak is the interference peak that appeared here prior to the detonation, the discussion above, of the temporal behavior of the background spectrum, suggests that the interference peak is subordinate at least during the intervals shown in Figures 3c-3e.

The overall appearance of the spectra in Figures 3c-3e is that of a continuous emission spectrum with attenuation bands at $\omega = n\ \Omega_{ci}$. The existance of a continuous spectrum as opposed to a line spectrum requires oblique propagation. Tataronis and Crawford[7] have computed dispersion curves for oblique propagation in a collisionless Maxwellian plasma. They find that very strong damping occurs at propagation angles appreciably less than 90 deg to the magnetic field. They also find that the real frequencies occupy a larger portion of the passband when damping is included. The spectrum would ideally consist of passbands between and separated from $\omega = n\ \Omega_{ci}$, with weak damping on the low side of the passband and strong damping on the high side.

Without detailed measurements of the particle density and velocity space distributions it would be presumptuous to attribute the waves to a specific mechanism.

Such waves can be excited by a variety of anisotropies including gradient effects in which the waves are excited by finite Larmor currents.[8]

REFERENCES

[1]M. C. Kelley, A. Pedersen, U. V. Fahleson, D. Jones, and D. Köhn, J. Geophys. Res. 79, 2859 (1974).

[2]G. M. Jenkins, and D. G. Watts, Spectral Analysis and its Applications (Holden Day, San Francisco, 1968).

[3]Morris B. Pongratz, Gordon M. Smith, C. Dexter Sutherland, John Zinn, Patrick Daly, Brian A. Whalen, and Timothy E. Eastman, Trans. Am. Geophys. Un. 58, 455 (1977).

[4]R. W. Motley, and N. D'Angelo, Phys. Fluids 6, 296 (1963).

[5]M. Porkolab, and G. S. Kino, Stanford University, Institute for Plasma Research Report No. SUIPR 23 (1965).

[6]H. W. Hendel, and M. Yamada, Phys. Rev. Letters 33, 1076 (1974).

[7]J. A. Tataronis, and F. W. Crawford, Stanford University, Institute for Plasma Research Report No. SUIPR 27 (1965).

[8]A. B. Mikhailovskii, Theory of Plasma Instatilities Vol. 2: Instabilities of an Inhomogeneous Plasma, (Consultants Bureau, New York, New York, 1974).

THE IVAN A. GETTING LABORATORIES

The Laboratory Operations of The Aerospace Corporation is conducting experimental and theoretical investigations necessary for the evaluation and application of scientific advances to new military concepts and systems. Versatility and flexibility have been developed to a high degree by the laboratory personnel in dealing with the many problems encountered in the nation's rapidly developing space and missile systems. Expertise in the latest scientific developments is vital to the accomplishment of tasks related to these problems. The laboratories that contribute to this research are:

Aerophysics Laboratory: Launch and reentry aerodynamics, heat transfer, reentry physics, chemical kinetics, structural mechanics, flight dynamics, atmospheric pollution, and high-power gas lasers.

Chemistry and Physics Laboratory: Atmospheric reactions and atmospheric optics, chemical reactions in polluted atmospheres, chemical reactions of excited species in rocket plumes, chemical thermodynamics, plasma and laser-induced reactions, laser chemistry, propulsion chemistry, space vacuum and radiation effects on materials, lubrication and surface phenomena, photosensitive materials and sensors, high precision laser ranging, and the application of physics and chemistry to problems of law enforcement and biomedicine.

Electronics Research Laboratory: Electromagnetic theory, devices, and propagation phenomena, including plasma electromagnetics; quantum electronics, lasers, and electro-optics; communication sciences, applied electronics, semiconducting, superconducting, and crystal device physics, optical and acoustical imaging; atmospheric pollution; millimeter wave and far-infrared technology.

Materials Sciences Laboratory: Development of new materials; metal matrix composites and new forms of carbon; test and evaluation of graphite and ceramics in reentry; spacecraft materials and electronic components in nuclear weapons environment; application of fracture mechanics to stress corrosion and fatigue-induced fractures in structural metals.

Space Sciences Laboratory: Atmospheric and ionospheric physics, radiation from the atmosphere, density and composition of the atmosphere, aurorae and airglow; magnetospheric physics, cosmic rays, generation and propagation of plasma waves in the magnetosphere; solar physics, studies of solar magnetic fields; space astronomy, x-ray astronomy; the effects of nuclear explosions, magnetic storms, and solar activity on the earth's atmosphere, ionosphere, and magnetosphere; the effects of optical, electromagnetic, and particulate radiations in space on space systems.

THE AEROSPACE CORPORATION
El Segundo, California